Distributed Voltage Unbalance Compensation in Islanded Microgrids by Using Dynamic-Consensus-Algorithm

Meng, Lexuan; Zhao, Xin; Tang, Fen; Savaghebi, Mehdi; Dragicevic, Tomislav; Vasquez, Juan Carlos; Guerrero, Josep M.

Published in:
I E E E Transactions on Power Electronics

DOI (link to publication from Publisher):
10.1109/TPEL.2015.2408367

Publication date:
2016

Document Version
Early version, also known as pre-print

L. Meng, X. Zhao, F. Tang, M. Savaghebi, T. Dragicevic, J. C. Vasquez, and J. M. Guerrero, "Distributed voltage unbalance compensation in islanded microgrids by using dynamic-consensus-algorithm," IEEE Transactions on Power Electronics, 2015.

Distributed Voltage Unbalance Compensation in Islanded Microgrids by Using Dynamic-Consensus-Algorithm

Lexuan Meng, Xin Zhao, Fen Tang, Mehdi Savaghebi, Tomislav Dragicevic,
Juan C. Vasquez, *Senior Member*, *IEEE*, and Josep M. Guerrero, *Fellow*, *IEEE*

***Abstract*--In islanded microgrids (MGs), distributed generators (DGs) can be employed as distributed compensators for improving the power quality in the consumer side. Two-level hierarchical control can be used for voltage unbalance compensation. Primary level, consisting of droop control and virtual impedance, can be applied to help the positive sequence active and reactive power sharing. Secondary level is used to assist voltage unbalance compensation. However, if distribution line differences are considered, the negative sequence current cannot be well shared among DGs. In order to overcome this problem, this paper proposes a distributed negative sequence current sharing method by using a dynamic consensus algorithm (DCA). In clear contrast with the previously proposed methods, this approach does not require a dedicated central controller and the communication links are only required between neighboring DGs. The method is based on the modeling and analysis of the unbalanced system. Experimental results from an islanded MG system consisting of three 2.2 kVA inverters are shown to demonstrate the effectiveness of the method.**

***Index Terms*--Islanded microgrid, hierarchical control, voltage unbalance compensation, consensus algorithm, current sharing**

I. Introduction

The MicroGrid (MG) concept has been proposed for efficient and flexible utilization of distributed energy resources [1]. According to the US Department of Energy (DOE), as well as Electric Power Research Institute (EPRI), a MG is a group of interconnected loads and distributed energy resources within clearly defined electrical boundaries that acts as a single controllable entity with respect to the grid and that connects and disconnects from such grid to enable it to operate in both grid-connected or "island" mode. In that way, it provides a more flexible and reliable energy system. In order to achieve this ideal, several critical issues have to be properly addressed especially under islanded mode including system stability, power quality, distributed generator (DG) coordination, power sharing, energy management, etc. In case of power quality issues, the existence of single-phase loads may incur voltage unbalance causing instability and additional power losses. Series or shunt active power filters [2]–[9] are conventional solutions for unbalance compensation.

In case of MG system, in order to save the investment for extra compensation equipment, DGs can be employed as distributed active filters or compensators. This capability is enabled by prevalent utilization of interfacing inverters and the advanced sensing, monitoring and communication techniques [10]–[21]. A hierarchical control is proposed in [10] and [11] to compensate voltage unbalance in sensitive load bus of an islanded MG. The hierarchy consists of two levels: primary (*local*) and secondary (*central*). A compensating reference is generated by the secondary controller and sent to primary controller. Then, every primary controller follows the compensating reference and controls the DG to compensate unbalances in the point of common coupling. A negative sequence impedance controller has been proposed in [12] for islanded operation of medium voltage MG system realizing negative sequence current minimization so as to reduce the system unbalances. In [13], a central power sharing and voltage regulation method is proposed for achieving both the accurate power sharing and enhanced voltage quality in terms of harmonics, disturbances and unbalances, and the compensation commands are distributed to localized DGs through low bandwidth communication links (LBCL). Similar functions are also realized and discussed in [14]–[21] by properly controlling and coordinating the operation of power converter interfaced DGs. Moreover, in order to make DGs share the total power considering both negative sequence quantities and harmonic currents, several methods have been studied. Centralized control, such as the cases presented in [13], [21], is a conventional way to achieve the accurate total power sharing. However, under distributed generation, storage and consumption paradigm, centralized control is facing obstacles because of the high communication and implementation cost, limited flexibility and low reliability due to its single point of failure feature. In order to achieve better power quality as well as reactive power and harmonic current sharing, a coordinated control strategy based on detecting and limiting the harmonic and reactive conductance and susceptance by using Fryze-Buchholz-Dpenbrock theory is proposed in [14].

In recent years, with the advance of information and communication technologies, distributed control methods have

L. Meng, X. Zhao, M. Savaghebi, T. Dragicevic, J. C. Vasquez, J. M. Guerrero are with Department of Energy Technology, Aalborg University, 9220 Aalborg, Denmark (e-mail: lme@et.aau.dk; xzh@et.aau.dk; mes@et.aau.dk; tdr@et.aau.dk; juq@et.aau.dk; joz@et.aau.dk).

F. Tang is with National Active Distribution Network Technology Research Center, Beijing Jiaotong University, Beijing, China (e-mail: ftang_nego@126.com).

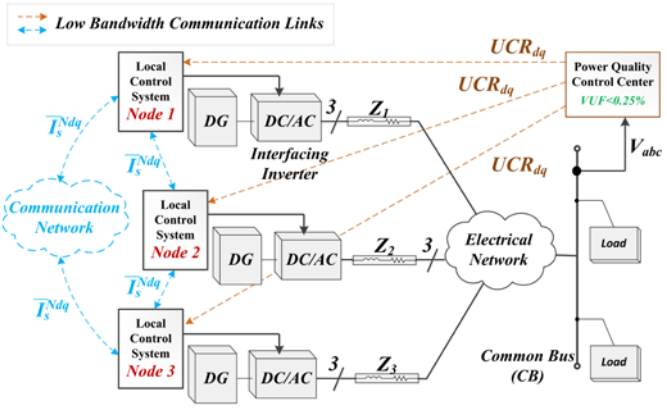

Fig. 1. Single line representation of a 3-phase islanded MG.

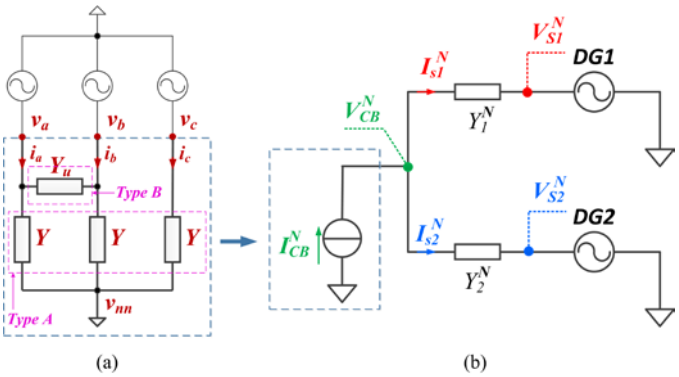

Fig. 2. Unbalanced system modeling: (a) Unbalanced load equivalent circuit in 3-phase 3-wire system; (b) Negative sequence equivalent circuit.

been more and more studied and applied in MG related research works. Consensus algorithms have been mostly used as they offer effective information sharing among distributed agents, facilitating in that way the distributed coordination and control of DGs. For instance, the authors of [22] propose gossip algorithm based distributed secondary control for voltage and frequency restoration in an islanded MG. Based on consensus algorithm, similar approach is applied in MGs for frequency recovery purposes [23].

In order to realize accurate current sharing among DGs while also ensure voltage unbalance compensation, this paper proposes a dynamic consensus algorithm (DCA) based negative sequence current sharing method forming a distributed hierarchical control scheme. The advantages of the proposed approach include: 1) it does not require a dedicated central controller; 2) communication links are only required between neighboring units; 3) plug-and-play functions can be realized achieving more flexible and reliable operation.

The study case system is introduced in Section II along with analysis of the unbalance compensation and negative sequence current sharing approach. The distributed hierarchical control scheme and detailed control system are presented in Section III. Section IV gives details regarding the DCA and its dynamics. dSPACE system based experimental results are shown in Section V to verify the validity of the proposed approach. Section VI presents the conclusion.

II. Unbalanced Islanded MG Analysis

In a three-phase islanded MG shown in Fig. 1, several DGs are installed to supply a common bus (CB). A power quality control center (PQCC) is established for taking care of power quality issues, such as voltage unbalance and harmonics. If unbalanced loads are connected on CB, voltage unbalance may appear. The PQCC measures the three-phase voltage on CB and calculates the voltage unbalance factor (VUF) [24], [25]. Based on the allowable VUF limits on CB, the PQCC generates unbalance compensation references in *d-q* reference (UCR_{dq}) and sends them through LBCLs to DG units, and employs DGs as distributed compensators [10]. The local control systems (LC) follow the UCR_{dq} and provide compensation support to the system. However, if the impedances between DGs and CB are different because of different types and lengths of distribution lines, the same compensation values will cause unequal negative sequence current sharing. In this situation, the DG units located closer to CB will automatically supply more current which may cause overloading of these DGs, especially under heavy load conditions. Therefore, in order to derive a method that is able to realize proper compensation efforts sharing, a model of the unbalanced system needs to be established first.

A. Unbalanced System Analysis

Assuming the presence of unbalanced loads on CB, as that shown in Fig. 2 (a), the symmetrical components of the system can be calculated based on classical methods [25]:

$$\begin{cases} Y_{ss} = A^{-1} \cdot Y_{ph} \cdot A \\ V_{ss} = A^{-1} \cdot V_{ph} \\ I_{ss} = Y_{ss} \cdot V_{ss} \end{cases} \tag{1}$$

where Y_{ss}, V_{ss} and I_{ss} are respectively the admittance matrix, voltage and current in symmetrical system, Y_{ph} and V_{ph} are respectively the admittance matrix and phase voltage in 3-phase system:

$$Y_{ph} = \begin{bmatrix} Y+Y_u & -Y_u & 0 \\ -Y_u & Y+Y_u & 0 \\ 0 & 0 & Y \end{bmatrix}; V_{ph} = \begin{bmatrix} V_a - V_{nn} \\ V_b - V_{nn} \\ V_c - V_{nn} \end{bmatrix} \tag{2}$$

and A is the transformation matrix between 3-phase system and symmetrical system (a used in the following equations is equal to $1\angle 120°$):

$$A = \begin{bmatrix} 1 & 1 & 1 \\ 1 & a^2 & a \\ 1 & a & a^2 \end{bmatrix} \tag{3}$$

The positive and negative sequence currents can be obtained by solving (1):

$$\begin{cases} \dot{I}^P = \dot{V}^P \cdot Y + (\dot{V}^P - a \cdot \dot{V}^N) \cdot Y_u \\ \dot{I}^N = \dot{V}^N \cdot Y + (\dot{V}^N - a^2 \cdot \dot{V}^P) \cdot Y_u \end{cases} \tag{4}$$

where $\dot{I}$ and $\dot{V}$ are respectively the current and voltage phasors, the superscripts P and N denote the positive- and negative-sequence quantities respectively. Y and Y_u are the admittances denoted as *Type A* and *Type B* loads, as shown in Fig. 2 (a). In addition, considering the fact that the maximum allowed voltage unbalance in power systems is 3% as defined by *ANSI C84.1-1995* [26], the positive sequence voltage is much larger than negative sequence voltage. When *VUF* value

is within the range 0-5%, the value of the term $\dot{V}^N \cdot Y + \dot{V}^N \cdot Y_u$ is always less than 5% of the nominal positive sequence current, which can be neglected even under the condition that Y is much larger than Y_u. Accordingly, (4) can be well approximated as:

$$\begin{cases} \dot{I}^P \approx \dot{V}^P \cdot Y + \dot{V}^P \cdot Y_u \\ \dot{I}^N \approx -a^2 \cdot \dot{V}^P \cdot Y_u \end{cases} \quad (5)$$

It can be seen from (5) that the negative sequence current is determined by the positive sequence voltage $\dot{V}^P$ and unbalanced load Y_u. In addition, as the voltage variation is bounded within 5% according to *IEEE Std 1547-2003* [27], the unbalanced load can be seen as a current source (see I_{CB}^N in Fig. 2 (b)) under a certain load condition.

B. Voltage Unbalance Compensation and Negative Sequence Current Sharing Approach

Based on exemplary system shown in Fig. 2 (b), the aim of voltage unbalance compensation strategy is actually to reduce the negative sequence voltage on CB (V_{CB}^N). The ideal compensation process is sketched in Fig. 3 (a). Ohm's law is also obeyed in the negative sequence equivalent circuit:

$$\begin{cases} \dot{V}_{CB}^N = \dot{V}_{S1}^N + \dot{I}_{S1}^N / Y_1^N \\ \dot{V}_{CB}^N = \dot{V}_{S2}^N + \dot{I}_{S2}^N / Y_2^N \\ \dot{I}_{CB}^N = \dot{I}_{S1}^N + \dot{I}_{S2}^N \end{cases} \quad (6)$$

where $\dot{V}_{S1}^N$ and $\dot{V}_{S2}^N$ are the negative sequence voltage phasors at DG sides, $\dot{I}_{CB}^N$, $\dot{I}_{S1}^N$ and $\dot{I}_{S2}^N$ are the negative sequence current phasors, Y_1^N and Y_2^N are the admittances of distribution lines. As $\dot{I}_{CB}^N$ can be seen as a constant variable if unbalanced load Y_u remains unchanged, $\dot{V}_{CB}^N$ can be reduced to $\dot{V}_{CB}^{N'}$ by decreasing the negative sequence voltage in DG sides (from $\dot{V}_{S1}^N, \dot{V}_{S2}^N$ to $\dot{V}_{S1}^{N'}, \dot{V}_{S2}^{N'}$, respectively), as shown in Fig. 3 (a). In addition, if $\dot{V}_{S1}^N$ and $\dot{V}_{S2}^N$ are equally adjusted ($\dot{V}_{S1}^{N'} = \dot{V}_{S2}^{N'}$), the negative sequence current flow $\dot{I}_{S1}^N$ and $\dot{I}_{S2}^N$ will remain unchanged. By applying this approach, the voltage unbalance on CB can be controlled to a relative lower level in order to keep the good power quality. However, it can be also seen from Fig. 3 (a) that the negative sequence current is not well shared if the distribution line admittances are different. With the same compensation references, the DG unit with larger admittance will provide more current which may cause overcurrent fault. Accordingly, it is better to make the DGs share the negative sequence current according to their power ratings so as to ensure the safe operation especially under severe unbalance conditions.

The simplified process of this method is sketched in Fig. 3 (b). It can be seen that by properly adjusting DG compensation references (from $\dot{V}_{S1}^{N'}, \dot{V}_{S2}^{N'}$ to $\dot{V}_{S1}^{N''}, \dot{V}_{S2}^{N''}$, respectively), the negative sequence current sharing proportion can be equalized ($\dot{I}_{S1}^{N''} = \dot{I}_{S2}^{N''}$) without affecting the desired negative sequence voltage on CB ($\dot{V}_{CB}^{N'}$). Based on this approach, this paper proposes an additional control loop to improve the negative sequence current sharing. The complete hierarchical control scheme is presented in the Section III.

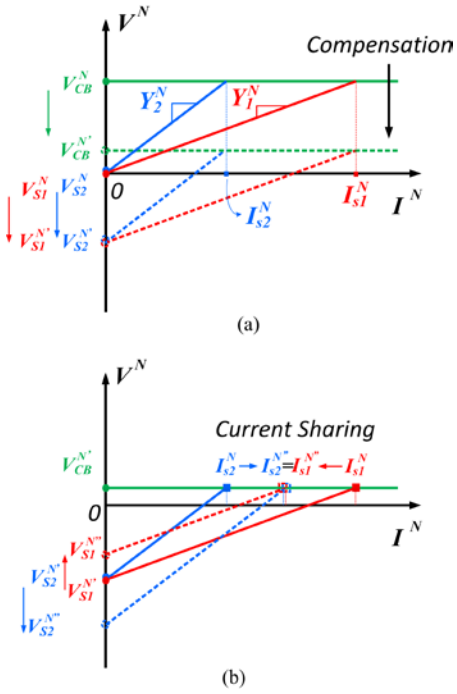

Fig. 3. (a) Simplified voltage unbalance compensation approach; (b) Simplified negative sequence current sharing approach.

III. Hierarchical Control Scheme

In this paper, the islanded MG is considered as several voltage sourced converters (VSC) connected to a common bus through *LC* filters and distribution lines (Y_i), as shown in Fig. 4. The energy resources are modeled as DC voltage links input to the VSCs. A hierarchical control is proposed including primary and secondary control levels as well as a communication layer.

A. Primary Control Loops

The primary control includes current and voltage control loops, active and reactive power droop control loops and virtual impedance loops. All the control loops are designed in $\alpha\beta$ frame. Since the DGs and the system are operating in islanded mode, P^+/f and Q^+/V based droop control is used for coordinating the operation of those DGs which mimic the behavior of synchronous generators in conventional power system to achieve positive sequence active and reactive power sharing [10], [28]. Accordingly, the voltage and frequency at CB is regulated by the droop control. As shown in Fig. 4, the positive sequence output active and reactive power of the inverter is first calculated based on the instantaneous power theory [29]. Positive sequence active and reactive power (P^+ and Q^+) can be extracted by using *low pass filters* (LPF). The calculated P^+ and Q^+ are then used by droop controller to generate voltage and frequency references.

In addition to droop control, a virtual impedance loop [10], [28] is implemented so as to ensure decoupling of P and Q, and to make the system more damped without inducing additional losses.

In order to track non-dc variables, proportional-resonant (PR) controllers are used in the voltage and current control

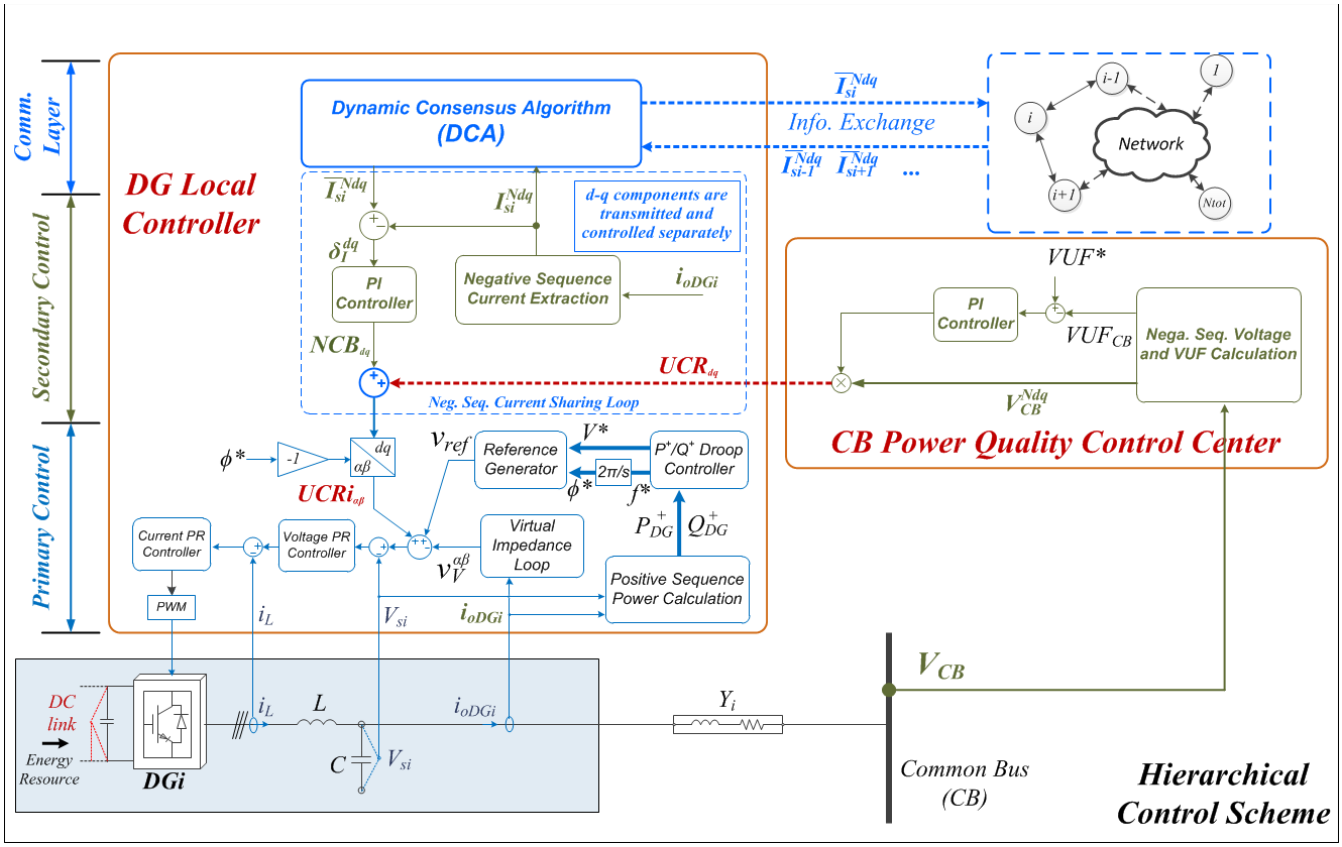

Fig. 4. Proposed hierarchical control scheme.

loops [10], [28]. More details about the primary control and inner control loops can be found in [10].

B. Secondary Voltage Unbalance Compensation

The secondary control loop in the power quality control center deals with CB voltage unbalance compensation by sending Unbalance Compensation Reference (UCR_{dq}) to local controllers through LBCL. As shown in Fig. 4, the CB voltage is first measured and the positive- and negative sequence components in *d-q* reference are extracted. Voltage unbalance factor (*VUF*) at CB can be calculated as follows [24]:

$$VUF_{CB} = 100 \cdot \sqrt{\frac{(v_{CB}^{Nd})^2 + (v_{CB}^{Nq})^2}{(v_{CBd}^{Pd})^2 + (v_{CB}^{Pq})^2}} \tag{7}$$

Then the error between calculated *VUF* and reference VUF^* is fed to a proportional-integral (PI) controller. The output of *PI* controller is multiplied by v_{CB}^{Ndq} to generate the common compensation reference UCR_{dq} [10].

In each local primary controller, the UCR_{dq} is transformed to $\alpha\beta$ frame where $-\phi^*$ is used as the rotation angle as the transformation is executed over negative sequence values.

C. Secondary Negative Sequence Current Sharing Control

In order to improve the negative sequence current sharing, the negative sequence current sharing loop compares the *d-q* components of local negative sequence current (I_{si}^{Ndq}) with averaged values of *d-q* components of the negative sequence current from all the DG sides ($\overline{I}_{si}^{Ndq}$):

$$NCB_{dq} = \left(\frac{k_{isc}^{dq}}{s} + k_{psc}^{dq}\right) \cdot \left(\overline{I}_{si}^{Ndq} - I_{si}^{Ndq}\right) \tag{8}$$

where k_{psc}^{dq} and k_{isc}^{dq} are the proportional and integral coefficients of the PI control loop for *d*- and *q*-axis currents respectively (*d*- and *q*-axis currents are controlled separately), I_{si}^{Ndq} is the locally measured negative sequence current in *d-q* reference, and $\overline{I}_{si}^{Ndq}$ is the average negative sequence current discovered by using DCA. It needs to be clarified that for DGs with different power ratings, the negative sequence current of each DG can be normalized to obtain the per unit (p.u.) value. Then instead of using real value, the p.u. value can be used in the negative sequence current sharing loop and dynamic consensus algorithm in Fig. 4 so as to make DGs proportionally share the total load current according to their power ratings. But for simplification, the DGs are considered to have the same capacity and real values are used along this paper so as to clearly show the convergence of negative sequence current and accurate sharing of total output current.

The next Section is dedicated to the fundamentals of DCA and details of its application to the proposed control scheme.

IV. Dynamic Consensus Algorithm

A. Consensus Algorithm Fundamentals

Consensus problems have their roots in the computer science area [30]. In recent years, they have been more and more applied in multi-agent and multi-vehicle systems with aim of facilitating the coordination among large number of distributed agents/vehicles [23], [31]–[34]. The general purpose of consensus algorithm is to allow a set of distributed agents to reach an agreement on a quantity of interest by

exchanging information through communication network. In case of MG systems, these algorithms can achieve the information sharing and coordination among distributed generators, consumers and storage systems. *Graph Laplacians* [35] describe the underlying communication structure in these kinds of systems and play a pivotal role in their convergence and dynamic analysis.

Considering the discrete nature of communication data transmission, the discrete form of consensus algorithm is considered in this paper. The fundamental can be presented as [31], [36]:

$$x_i(k+1) = x_i(k) + \varepsilon \cdot \sum_{j \in N_i} a_{ij} \cdot (x_j(k) - x_i(k)) \tag{9}$$

where $x_i(k)$ is the information status of agent i at iteration k, and a_{ij} is the connection status between node i and node j. In that sense, if the nodes i and j are not neighboring, then a_{ij} =0. N_i is the set of indices of the agents that are connected with agent i, ε is the constant edge weight used for tuning the dynamic of DCA.

In addition, in order to ensure the convergence of consensus to accurate value in dynamically changing environment, a modified version of the algorithm, referred to as dynamic consensus algorithm [37], is applied in this paper (see Fig. 5):

$$x_i(k+1) = x_i(0) + \varepsilon \cdot \sum_{j \in N_i} \delta_{ij}(k+1) \tag{10}$$

$$\delta_{ij}(k+1) = \delta_{ij}(k) + a_{ij} \cdot \left(x_j(k) - x_i(k)\right) \tag{11}$$

where $\delta_{ij}(k)$ stores the cumulative difference between two agents, and $\delta_{ij}(0) = 0$. Based on (10) and (11), it is explicit that the final consensus value will be reached regardless of any changes to $x_i(0)$.

From a system point of view, the vector form of the iteration algorithm can be expressed as [31]:

$$\mathbf{x}(k+1) = \mathbf{W} \cdot \mathbf{x}(k) \tag{12}$$

with $\mathbf{x}(k) = [x_1(k), x_2(k), ..., x_{n_T}(k)]^T$ and $\mathbf{W}$ is the weight matrix of the communication network. If constant edge weight ε is considered, $\mathbf{W}$ can be described as:

$$\mathbf{W} = \mathbf{I} - \varepsilon \cdot \mathbf{L} \tag{13}$$

$$\mathbf{L} = \begin{bmatrix} \sum_{j \in N_1} a_{1j} & \cdots & -a_{1n_T} \\ \vdots & \ddots & \vdots \\ -a_{1n_T} & \cdots & \sum_{j \in N_{n_T}} a_{n_T j} \end{bmatrix} \tag{14}$$

where $\mathbf{L}$ is the *Laplacian matrix* of the communication network [38], [39], n_T is the total number of agents. The final consensus equilibrium $\mathbf{x}_{eq}$ is:

$$\mathbf{x}_{eq} = \lim_{k \to \infty} \mathbf{x}(k) = \lim_{k \to \infty} \mathbf{W}^k \mathbf{x}(0) = \left(\frac{1}{n_T} \mathbf{1} \cdot \mathbf{1}^T \right) \mathbf{x}(0) \tag{15}$$

where $\mathbf{x}(0) = [\mathbf{x}_1(0), \mathbf{x}_2(0), ..., \mathbf{x}_{N_T}(0)]$ is the vector of the initial values held by each agent, $\mathbf{1}$ denotes the vector with the values of all the elements being 1. The detailed proof of the convergence can be found in [31].

In this study case, $\mathbf{x}(k)$ includes the discovered average value of negative sequence current in *d-q* references ($\bar{I}_{si}^{Ndq}$), and $\mathbf{x}(0)$ is the local measured negative sequence current

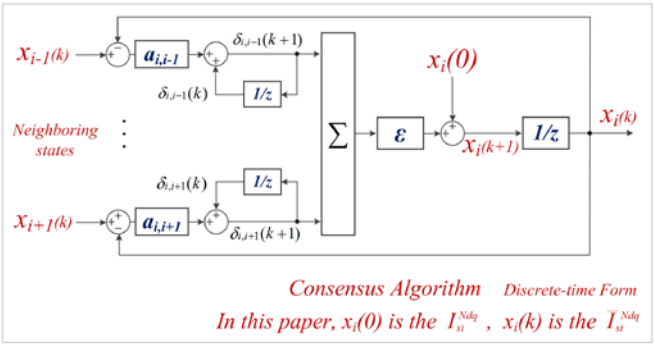

Fig. 5. Dynamic Consensus Algorithm.

(I_{si}^{Ndq}). Accordingly, DCA helps each local unit to discover the global average of negative sequence current.

B. Consensus Algorithm Dynamics

As the constant weight ε defines the dynamics of the algorithm, it has to be properly chosen to ensure the fast and stable convergence of the algorithm. It is demonstrated in [40] that the fastest convergence can be obtained when the spectral radius (ρ) of matrix $W - (1/n_T) \cdot \mathbf{1} \cdot \mathbf{1}^T$ is minimized. The optimal that offers the fastest convergence speed can be calculated as:

$$\varepsilon = \frac{2}{\lambda_1(\mathbf{L}) + \lambda_{n-1}(\mathbf{L})} \tag{16}$$

where $\lambda_j(\cdot)$ denotes the j^{th} largest eigenvalue of a symmetric matrix. In the study case MG, a bidirectional communication network is established in which the three local control systems communicate with their neighboring systems.

Taking ring-shape communication topology as an example, the *Laplacian matrix* is defined as:

$$\mathbf{L} = \begin{bmatrix} 2 & -1 & -1 \\ -1 & 2 & -1 \\ -1 & -1 & 2 \end{bmatrix} \tag{17}$$

the eigenvalues of which are $[0\ 3\ 3]^T$. According to $\mathbf{L}$ and its eigenvalues, the optimal $\varepsilon = 1/3$. A convergence speed comparison is shown in Fig. 6 (a), where the constant edge weight ε is changed from 0.02 to 0.6. It can be seen from the four figures in Fig. 6 (a) that when $\varepsilon = 1/3$ the distributed agents obtain fastest convergence speed.

Moreover, one of the most important objectives of applying DCA is to realize plug-and-play capability. The performance of DCA with online including/excluding units is shown in Fig. 6 (b). The three units start with initial value [0 2 7] and first converge to average value. At 1s, one of the units stops communicating with the other two. The other two units are able to find a new averaging value between them while the excluded one restores to its initial value. At 2s, the communication links are recovered and the three units converge to the averaging value again.

V. Experimental Results

The proposed MG power stage and control scheme is implemented at the *intelligent Microgrid Lab* of Aalborg University [41], as the experimental setup shown in Fig. 7. The

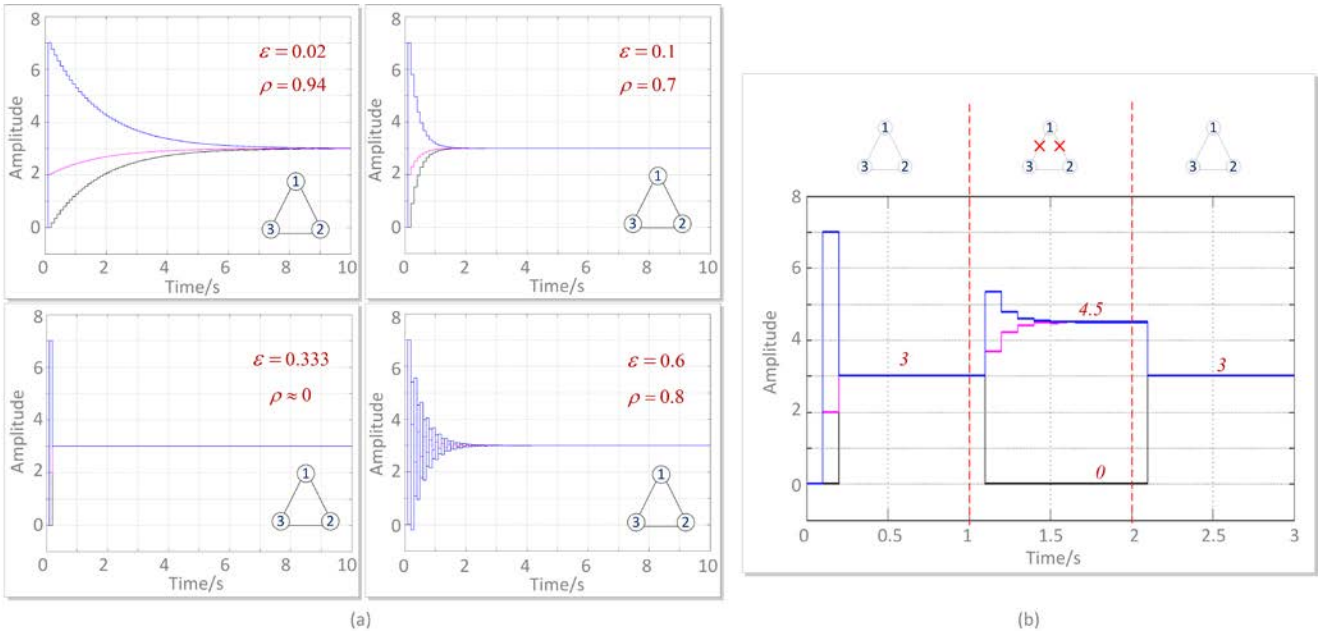

Fig. 6. Consensus algorithm dynamics: (a) with different constant edge weight; (b) with online including/excluding units.

TABLE I. POWER STAGE AND MG PLANT PARAMETERS

DG Inverter Ratings	**Inverter Output Filter**		**Distribution Line Admittances (Positive Seq.)**			**Rated Voltage and Frequency**	
Power Rating (kW)	*L (mH)*	*C (μF)*	Y_1 *(S)*	Y_2 *(S)*	Y_3 *(S)*	*Voltage (V)*	*Frequency (Hz)*
2.2	*1.8*	*25*	*0.38- j1.32*	*0.38- j1.32*	*0.07- j0.47*	*220*	*50*

TABLE II. PRIMARY CONTROL PARAMETERS

Droop Controller					**Virtual Impedance**		**Voltage Controller**			**Current Controller**		
m_D((Hz · s)/W)	m_P(Hz/W)	n_P(V/VAr)	V_0 (V)	f_0(Hz)	R_v (Ω)	L_v (mH)	k_{pV}	k_{rV}	ω_{cV}	k_{pI}	k_{rI}	ω_{cI}
8e-5	*8e-5*	*0.01*	$220\sqrt{2}$	*50*	*1*	*4*	*0.5*	*5*	*2*	*0.7*	*500*	*2*

TABLE III. SECONDARY CONTROL AND CONSENSUS ALGORITHM PARAMETERS

Unbalance Compensation			**Negative Sequence Current Sharing**		**DCA Parameter**
k_{psv}	k_{isv}	*VUF*(%)*	k_{psc}^{dq}	k_{isc}^{dq}	ε
0.5	*7*	*0.25*	*2*	*2*	*1/3*

MG platform consists of three *Danfoss* inverters (three-leg three-phase 2.2kVA inverters with LCL filters) which are operating in parallel to emulate DGs. The detailed electrical configuration of each inverter and its output filter is shown in Fig. 4. Resistive loads are connected to CB to simulate different loading conditions. Control algorithm is developed in Simulink and compiled to dSPACE system to switch inverters. Detailed power stage and control system parameters can be found in Table I, II and III. In Table II, m_P and m_D are the proportional and derivative coefficients of active power droop controller, n_P is the proportional coefficient of reactive power droop controller, E_0 and ω_0 are the nominal voltage amplitude and angular frequency, R_V and L_V are the virtual resistance and inductance, k_{pV}, k_{rV} and k_{pI}, k_{rI} are the proportional and resonant coefficients, and ω_{cV} and ω_{cI} are the cut-off angular frequencies of the voltage and current controllers, respectively. In Table III, k_{psv} and k_{isv} are the proportional and integral

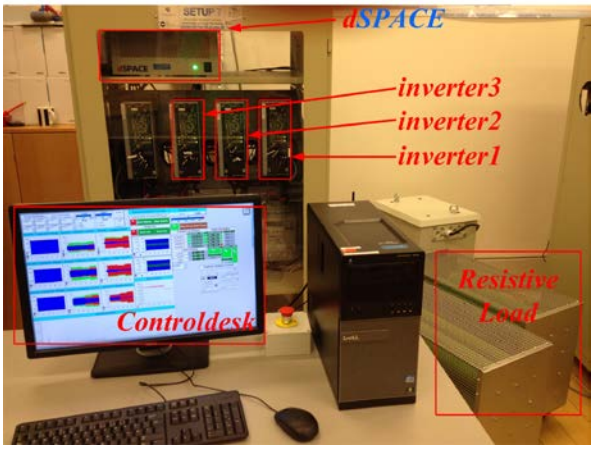

Fig. 7. Laboratory setup.

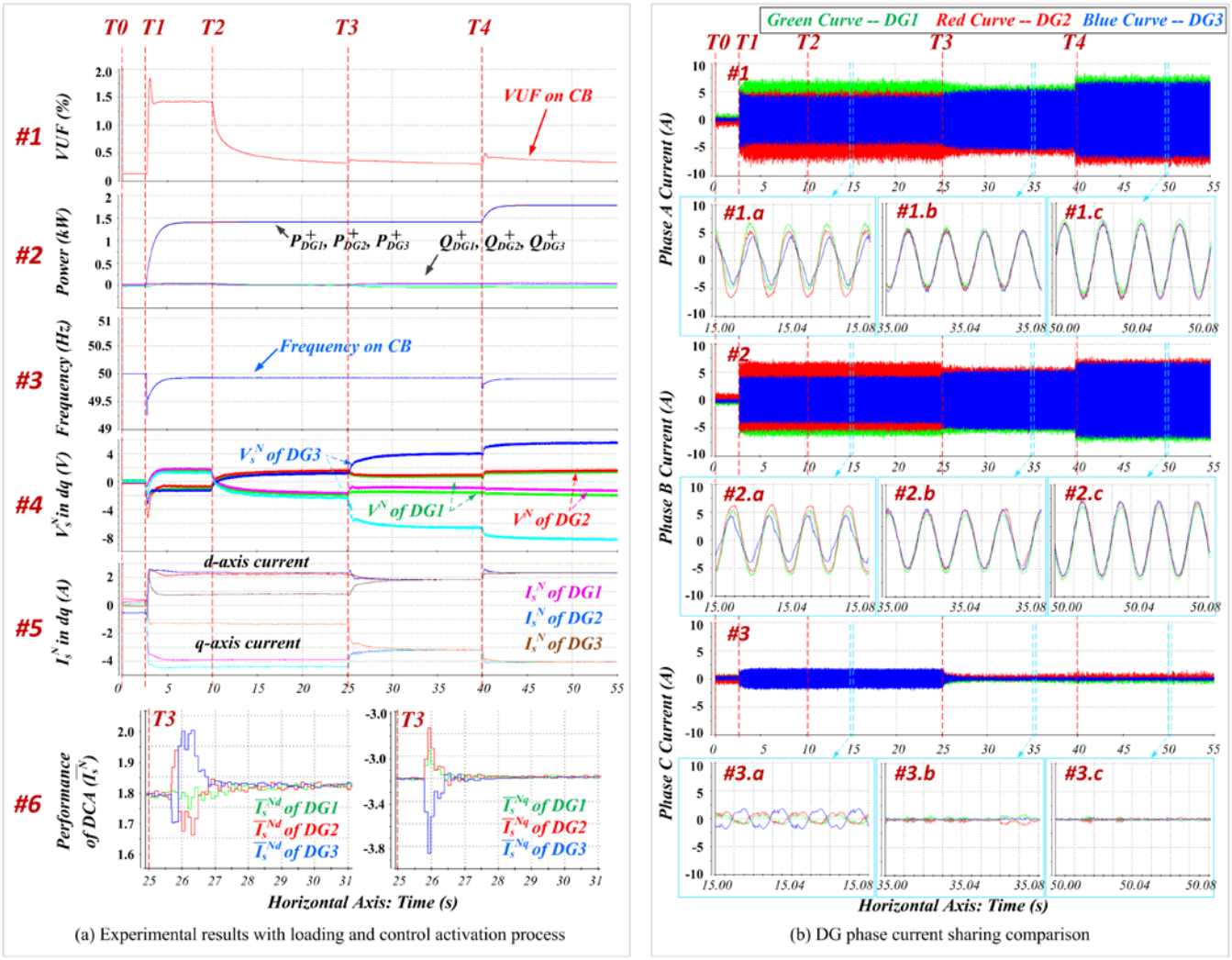

Fig. 8. (a) Experimental results with loading and control activation process; (b) DG phase current comparison.

coefficients of the voltage unbalance control loop, VUF^* is the reference.

During the starting phase, one of DGs first starts. Then the other DGs are connected to the CB by using typical PLL based synchronization control [28], where each DG measures and synchronizes with CB voltage before connecting to the CB. After all the DGs are connected to the CB, the following experiments are executed to test the performance of the system.

TABLE IV. LOADING AND ACTIVATION PROCESS

time	CB
T0	Type A: *Y=0.0022 S*
T1	Type B: Y_u*=0.03 S*
T2	Activate secondary unbalance compensation
T3	Activate negative sequence current sharing
T4	Type B: Y_u*=0.0044 S*

A. Activation and Loading Process

In order to test the performance of the system, a loading and control activation process is conducted as described in Table IV. The results are shown in Fig. 8 (a) and (b). Fig. 8 (a) shows the performance of the system, and Fig. 8 (b) compares the phase current of the three DGs (phase A, B and C are compared separately with green, red and blue curves denoting the three DGs).

At *T0*, a balanced resistive load is connected to the system. From *T0* to *T1*, the VUF on CB is in a low level (see Fig. 8 (a) #1), and only small amount of negative sequence voltage and current exist (see Fig. 8 (a) #4 and #5).

At *T1*, an unbalanced resistive load is connected, which causes the increasing of VUF on CB (see Fig. 8 (a) #1), also the positive sequence power and negative sequence current rise (see Fig. 8 (a) #2 and #5). The frequency deviation (see Fig. 8 #3) is caused by the using of droop control (P^+/f and Q^+/V droop). Droop control helps the automatic positive sequence power sharing. However, with the increasing of positive sequence power, frequency deviates from the nominal value (50Hz). A proper design of droop control parameters can keep the frequency within limited range given by specific grid standard. In addition, centralized or distributed secondary control can be implemented to eliminate the steady state error as was proposed in [22] and can be incorporated into the method proposed in this paper. Since the frequency secondary control is out of the scope of this paper and the proposed method does not have impact on system frequency (as shown

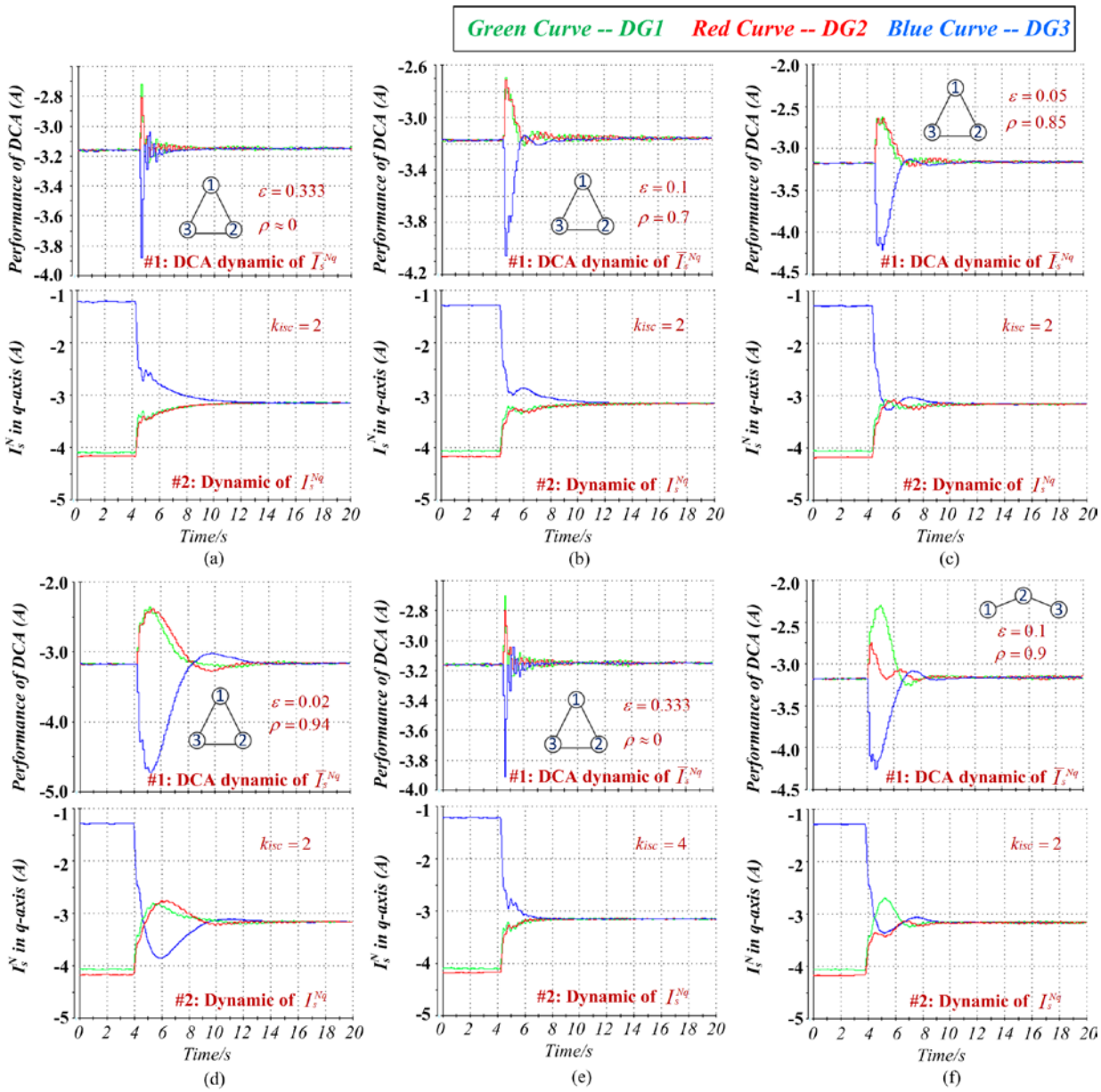

Fig. 9. Evaluation of DCA Effect: (a) ring-shape topology with $\varepsilon = 0.333$; (b) ring-shape topology with $\varepsilon = 0.1$; (c) ring-shape topology with $\varepsilon = 0.05$; (d) ring-shape topology with $\varepsilon = 0.02$; (e) line-shape topology with $\varepsilon = 0.333$; (f) line-shape topology with $\varepsilon = 0.1$.

in Fig. 8 (a) #3, at T3 the proposed control is activated but does not affect the system frequency), it is not considered in the experiment.

At *T2*, the secondary unbalance compensation control is activated. By adjusting the negative sequence voltage on DG sides the VUF on CB is reduced to a low level (see Fig. 8 (a) #1 and #4), while the positive sequence power and negative sequence current flow remains unchanged (see Fig. 8 (a) #2 and #5). Also the positive sequence power is well shared because of the using of droop control and virtual impedance loop. However, as the negative sequence current is not well shared, the phase currents of the three DGs have obvious differences, as shown in Fig. 8 (b) #1.a, #2.a and #3.a. This result is in accordance with the analysis in part B of Section III and Fig. 3 (a).

At *T3*, the negative sharing control is activated. The DCA first helps each local unit to find the averaging of negative sequence current. The dynamic of this process is shown in Fig. 8 (a) #6, the information obtained by each unit ($\bar{I}_{s1}^{Ndq}$, $\bar{I}_{s2}^{Ndq}$ and $\bar{I}_{s3}^{Ndq}$) converges to the same average value in less than 2s. By using this average value as the reference, the negative sequence current sharing loop helps the equalization of the DG currents by adjusting the negative sequence voltage on DG sides, as shown in Fig. 8 (a) #4 and #5. The detailed phase current comparison after activating the control is also shown in Fig. 8 (b) #1.b, #2.b and #3.b, which shows that this control loop helps the accurate sharing of phase currents. As expected, the VUF on CB is kept at a low level during this process.

At *T4*, an additional unbalanced load is connected to test the performance of the system under dynamic load change. After the loading, the power generation and negative sequence current of all the DGs are increased. The proposed control

scheme is able to keep the VUF on CB at the desired value while ensure the accurate sharing of total currents among DGs.

B. Evaluation of DCA Effect

As the negative sequence current sharing is facilitated by using DCA, the communication part certainly has influence over the system dynamics. Communication topology and constant edge weight (ε) are both decisive factors on communication dynamics. The dynamics and convergence of *q*-axis negative sequence current (I_s^{Nq}) under different communication configurations are taken as example as shown in Fig. 9 with green, red and blue curves denoting the 3 DGs.

Fig. 9 (a)-(d) compare the convergence of DCA and the dynamic of the *q*-axis current (I_s^{Nq}) under the same ring-shape topology but with different constant edge weight (ε). It is demonstrated in Fig. 6 that the DCA obtains fastest convergence when $\varepsilon = 0.333$. In accordance with that, it can be seen from #1 in Fig. 9 (a)-(d) that with the decreasing of ε the convergence time of DCA becomes longer incurring more oscillation in the I_s^{Nq}. Also it can be seen from Fig. 9 (c) that although the DCA has slower convergence speed compared with Fig. 9 (a), the I_s^{Nq} converges faster but with small oscillation.

The above results demonstrate that the dynamic of the communication algorithm has certain interaction with secondary controller, and a better parameter tuning and matching between the DCA and controller can improve the system dynamics. This conclusion can be further verified by comparing the system dynamic under different secondary parameters as shown in Fig. 9 (a) and (e). In Fig. 10 (e) the ε is kept at 0.333 while the secondary integral term k_{isc} is increased from 2 to 4. It can be seen from Fig. 9 (a) and (e) that the DCA dynamics remain the same (comparing #1 in both figures) while the I_s^{Nq} converges faster under k_{isc}=4 (comparing #2 in both figures).

Apart from parameter influence, Fig. 9 (b) and (f) compare the convergence of DCA and the dynamic of the *q*-axis current (I_s^{Ndq}) under different communication topologies (ring-shape and line-shape). It can be seen from Fig. 9 (f) that under line-shape communication topology, the accurate averaging can be also guaranteed and the I_s^{Ndq} can be well controlled and shared among DGs, however, the dynamic of the system occurs to be oscillating because of the relative slower convergence speed of DCA compared with ring-shape case.

The above results give hint that the secondary control speed has to be well tuned according to the communication transmission rate and DCA convergence speed. It can be more safe and stable to slow down the secondary control considering that the real world communication transmission rate can be variable and DCA may, in some cases, need longer time to find the accurate averaging.

C. Validation of Excluding/Including Units

The purpose of using DCA is to enhance the flexibility of the system which includes the capability of online excluding and including units. A process of excluding and including DG to share the negative sequence current is conducted as shown in Fig. 10. At *T'0*, the negative sequence current is not well

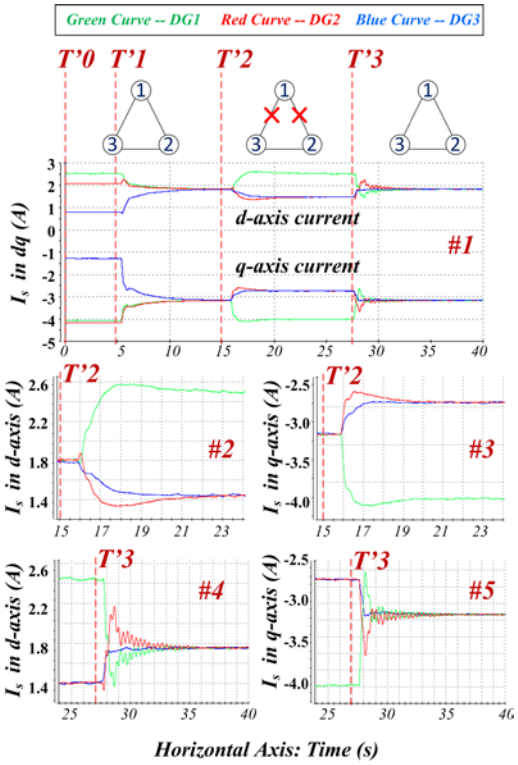

Fig. 10. Validation of excluding/including unit.

shared. At *T'1*, the negative sequence current sharing is activated. At *T'2*, DG1 is excluded from the sharing control in case of communication fault or intentional operation. It can be seen from Fig. 10 (during *T'2* to *T'3*) that the DG1 stops sharing the negative sequence current with the other two DGs while the other two DGs find the new averaging between them and continue sharing the negative sequence current. The dynamics during this process is shown in Fig. 10 #2 and #3 for *d*- and *q*-axis respectively. At *T'3*, DG1 is planned to re-join the current sharing. After this process, the total negative sequence current is accurately shared among the DGs again. The dynamics during this process is shown in Fig. 10 #4 and #5 for *d*- and *q*-axis respectively.

VI. Conclusion

This paper proposes a DCA based hierarchical control scheme to realize distributed negative sequence current sharing and voltage unbalance compensation. Although former studies realized voltage unbalance compensation, the negative sequence current cannot be well shared by only applying droop control, which may cause overcurrent condition for DGs located close to the CB. In order to improve the current sharing while considering the distributed fashion of future MG systems, this paper proposes a DCA based control method. An additional negative sequence current sharing loop is included. The unbalanced system is modeled with compensation and current sharing analysis. The proposed control scheme is implemented in a dSPACE based experimental setup to verify the effectiveness of the method. The results demonstrate that the proposed control scheme is able to realize voltage unbalance compensation while ensuring the accurate total current sharing among DGs. Also, the online

excluding/including unit processes are tested showing the enhanced system flexibility by applying such a scheme. Note that thanks to the distributed nature of the proposed approach, the controller does not need to be implemented in a centralized fashion, which may be dedicated to other management operations of the MG.

REFERENCES

[1] "IEEE Guide for Design, Operation, and Integration of Distributed Resource Island Systems with Electric Power Systems." pp. 1–54, 2011.

[2] D. Graovac, V. Katic, and A. Rufer, "Power Quality Problems Compensation With Universal Power Quality Conditioning System," *IEEE Trans. Power Deliv.*, vol. 22, no. 2, pp. 968–976, Apr. 2007.

[3] B. Singh, K. Al-Haddad, and A. Chandra, "A review of active filters for power quality improvement," *IEEE Trans. Ind. Electron.*, vol. 46, no. 5, pp. 960–971, 1999.

[4] A. Garcia-Cerrada, O. Pinzon-Ardila, V. Feliu-Batlle, P. Roncero-Sanchez, and P. Garcia-Gonzalez, "Application of a Repetitive Controller for a Three-Phase Active Power Filter," *IEEE Trans. Power Electron.*, vol. 22, no. 1, pp. 237–246, Jan. 2007.

[5] B. Singh and J. Solanki, "An Implementation of an Adaptive Control Algorithm for a Three-Phase Shunt Active Filter," *IEEE Trans. Ind. Electron.*, vol. 56, no. 8, pp. 2811–2820, Aug. 2009.

[6] F. Barrero, S. Martínez, F. Yeves, F. Mur, and P. M. Martínez, "Universal and reconfigurable to UPS active power filter for line conditioning," *IEEE Trans. Power Deliv.*, vol. 18, pp. 283–290, 2003.

[7] M. I. M. Montero, E. R. Cadaval, and F. B. Gonzalez, "Comparison of Control Strategies for Shunt Active Power Filters in Three-Phase Four-Wire Systems," *IEEE Trans. Power Electron.*, vol. 22, no. 1, pp. 229–236, Jan. 2007.

[8] S. George and V. Agarwal, "A DSP Based Optimal Algorithm for Shunt Active Filter Under Nonsinusoidal Supply and Unbalanced Load Conditions," *IEEE Trans. Power Electron.*, vol. 22, no. 2, pp. 593–601, Mar. 2007.

[9] T. Jin and K. M. Smedley, "Operation of One-Cycle Controlled Three-Phase Active Power Filter With Unbalanced Source and Load," *IEEE Trans. Power Electron.*, vol. 21, no. 5, pp. 1403–1412, Sep. 2006.

[10] M. Savaghebi, A. Jalilian, J. C. Vasquez, and J. M. Guerrero, "Secondary Control Scheme for Voltage Unbalance Compensation in an Islanded Droop-Controlled Microgrid," *IEEE Trans. Smart Grid*, vol. 3, no. 2, pp. 797–807, Jun. 2012.

[11] M. Savaghebi, A. Jalilian, J. C. Vasquez, and J. M. Guerrero, "Autonomous Voltage Unbalance Compensation in an Islanded Droop-Controlled Microgrid," *IEEE Trans. Ind. Electron.*, vol. 60, no. 4, pp. 1390–1402, Apr. 2013.

[12] M. Hamzeh, H. Karimi, and H. Mokhtari, "A New Control Strategy for a Multi-Bus MV Microgrid Under Unbalanced Conditions," *IEEE Trans. Power Syst.*, vol. 27, no. 4, pp. 2225–2232, Nov. 2012.

[13] M. Prodanovic and T. C. Green, "High-Quality Power Generation Through Distributed Control of a Power Park Microgrid," *IEEE Trans. Ind. Electron.*, vol. 53, 2006.

[14] Z. Zeng, R. Zhao, and H. Yang, "Coordinated control of multi-functional grid-tied inverters using conductance and susceptance limitation," *IET Power Electron.*, vol. 7, no. 7, pp. 1821–1831, Jul. 2014.

[15] J. A. Suul, A. Luna, P. Rodríguez, and T. Undeland, "Virtual-flux-based voltage-sensor-less power control for unbalanced grid conditions," *IEEE Trans. Power Electron.*, vol. 27, pp. 4071–4087, 2012.

[16] Z. R. Ivanović, E. M. Adžić, M. S. Vekić, S. U. Grabić, N. L. Čelanović, and V. A. Katić, "HIL evaluation of power flow control strategies for energy storage connected to smart grid under unbalanced conditions," *IEEE Trans. Power Electron.*, vol. 27, pp. 4699–4710, 2012.

[17] E. Jamshidpour, B. Nahid-Mobarakeh, P. Poure, S. Pierfederici, F. Meibody-Tabar, and S. Saadate, "Distributed Active Resonance Suppression in Hybrid DC Power Systems Under Unbalanced Load Conditions," *IEEE Transactions on Power Electronics*, vol. 28. pp. 1833–1842, 2013.

[18] A. Bueno, J. M. Aller, J. A. Restrepo, R. Harley, and T. G. Habetler, "Harmonic and Unbalance Compensation Based on Direct Power Control for Electric Railway Systems," *Power Electronics, IEEE Transactions on*, vol. 28. pp. 5823–5831, 2013.

[19] M. Reyes, P. Rodriguez, S. Vazquez, A. Luna, R. Teodorescu, and J. M. Carrasco, "Enhanced Decoupled Double Synchronous Reference Frame Current Controller for Unbalanced Grid-Voltage Conditions," *IEEE Trans. Power Electron.*, vol. 27, no. 9, pp. 3934–3943, Sep. 2012.

[20] S. Vazquez, J. A. Sanchez, M. R. Reyes, J. I. Leon, and J. M. Carrasco, "Adaptive vectorial filter for grid synchronization of power converters under unbalanced and/or distorted grid conditions," *IEEE Trans. Ind. Electron.*, vol. 61, pp. 1355–1367, 2014.

[21] L. Hang, B. Li, M. Zhang, Y. Wang, and L. M. Tolbert, "Equivalence of SVM and carrier-based PWM in three-phase/wire/level Vienna rectifier and capability of unbalanced-load control," *IEEE Trans. Ind. Electron.*, vol. 61, pp. 20–28, 2014.

[22] Q. Shafiee, C. Stefanovic, T. Dragicevic, P. Popovski, J. C. Vasquez, and J. M. Guerrero, "Robust Networked Control Scheme for Distributed Secondary Control of Islanded Microgrids," *IEEE Trans. Ind. Electron.*, vol. 61, no. 10, pp. 5363–5374, Oct. 2014.

[23] D. Wu, T. Dragicevic, J. C. Vasquez, J. M. Guerrero, and Y. Guan, "Secondary Coordinated Control of Islanded Microgrids Based on Consensus Algorithms," in *Proceedings of the 2014 IEEE Energy Conversion Congress and Exposition (ECCE)*, 2014, pp. 4290–4297.

[24] A. Jouanne and B. Banerjee, "Assessment of Voltage Unbalance," *IEEE Power Engineering Review*, vol. 21. pp. 64–64, 2001.

[25] J. D. Glover, M. Sarma, and T. Overbye, *Power System Analysis and Design*. 2011.

[26] "Electric Power Systems and Equipment—Voltage Ratings (60 Hertz)," *ANSI Stand. Publ. no. ANSI C84.1-1995*.

[27] "IEEE Standard for Interconnecting Distributed Resources with Electric Power Systems," *IEEE Std 1547-2003*, pp. 1–28, 2003.

[28] J. C. Vasquez, J. M. Guerrero, M. Savaghebi, J. Eloy-Garcia, and R. Teodorescu, "Modeling, analysis, and design of stationary-reference-frame droop-controlled parallel three-phase voltage source inverters," *IEEE Trans. Ind. Electron.*, vol. 60, pp. 1271–1280, 2013.

[29] H. Akagi, Y. Kanazawa, and A. Nabae, "Instantaneous Reactive Power Compensators Comprising Switching Devices without Energy Storage Components," *IEEE Trans. Ind. Appl.*, vol. IA-20, 1984.

[30] R. Olfati-Saber and R. M. Murray, "Consensus Problems in Networks of Agents With Switching Topology and Time-Delays," *IEEE Trans. Automat. Contr.*, vol. 49, no. 9, pp. 1520–1533, Sep. 2004.

[31] R. Olfati-Saber, J. A. Fax, and R. M. Murray, "Consensus and Cooperation in Networked Multi-Agent Systems," *Proc. IEEE*, vol. 95, 2007.

[32] Y. Xu and W. Liu, "Novel Multiagent Based Load Restoration Algorithm for Microgrids," *IEEE Trans. Smart Grid*, vol. 2, pp. 140–149, 2011.

[33] H. Liang, B. Choi, W. Zhuang, X. Shen, A. A. Awad, and A. Abdr, "Multiagent coordination in microgrids via wireless networks," *IEEE Wireless Communications*, vol. 19. pp. 14–22, 2012.

[34] L. Meng, T. Dragicevic, J. M. Guerrero, and J. C. Vasquez, "Dynamic consensus algorithm based distributed global efficiency optimization of a droop controlled DC microgrid." pp. 1276–1283, 2014.

[35] R. Merris, "Laplacian matrices of graphs: a survey," *Linear Algebra and its Applications*, vol. 197–198. pp. 143–176, 1994.

[36] A. Kashyap, T. Başar, and R. Srikant, "Quantized consensus," in *IEEE International Symposium on Information Theory - Proceedings*, 2006, pp. 635–639.

[37] M. Kriegleder, "A Correction to Algorithm A2 in 'Asynchronous Distributed Averaging on Communication Networks,'" vol. PP, no. 99. p. 1, 2013.

[38] N. Biggs, *Algebraic Graph Theory, Cambridge Tracks in Mathematics*. Cambridge, U.K.: Cambridge Univ. Press, 1974.

[39] C. Godsil and G. Royle, *Algebraic Graph Theory*, Vol. 207. New York: Springer-Verlag, 2001.

[40] L. X. L. Xiao and S. Boyd, "Fast linear iterations for distributed averaging," *42nd IEEE Int. Conf. Decis. Control (IEEE Cat. No.03CH37475)*, vol. 5, 2003.

[41] *Microgrid Research Programme*. URL: www.microgrids.et.aau.dk.

VII. BIOGRAPHIES

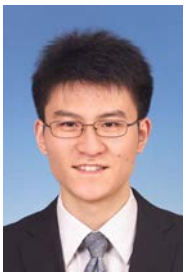

Lexuan Meng received the B.S. degree in Electrical Engineering and M.S. degree in Electrical Machine and Apparatus from Nanjing University of Aeronautics and Astronautics (NUAA), Nanjing, China, in 2009 and 2012, respectively. He is currently working toward his Ph.D. in power electronic systems at the Department of Energy Technology, Aalborg University, Denmark, as part of the Denmark Microgrids Research Programme (www.microgrids.et.aau.dk).
His research interests include the energy management system, secondary and tertiary control for microgrids concerning power quality regulation and optimization issues, as well as the applications of distributed control and communication algorithms.

Xin Zhao received the B.S. and M.S. degree in Power Electronics & Electrical Drives from Northwestern Polytechnical University, Xi'an, China, in 2010 and 2013, respectively. He is currently working toward the Ph.D. degree at Department of Energy Technology, Aalborg University, Denmark.
His research interests include control of power converters, power quality and microgrids.

Fen Tang received the B.S. degree in Electrical Engineering and the Ph.D. degree in Power Electronics & Electric Drives from Beijing Jiaotong University, Beijing, China, in 2006 and 2013, respectively. She is currently a Postdoc in Beijing Jiaotong University. From Jan. 2013 to Jan. 2014 she was a guest Postdoc at Department of Energy Technology, Aalborg University, Denmark.
Her research interests include microgrid, wind power generation system, power converter for renewable generation systems, power quality, and motor control.

Mehdi Savaghebi was born in Karaj, Iran, in 1983. He received the B.Sc. degree from University of Tehran, Iran, in 2004 and the M.Sc. and Ph.D. degrees with highest honors from Iran University of Science and Technology, Tehran, Iran in 2006 and 2012, respectively, all in Electrical Engineering. From 2007 to 2014, he was a Lecturer in Electrical Engineering Department, Karaj Branch, Islamic Azad University, Karaj, Iran, where he taught various courses and conducted research on power systems and electrical machines. In 2010, he was a Visiting Ph.D. Student with the Department of Energy Technology, Aalborg University, Aalborg, Denmark and with the Department of Automatic Control Systems and Computer Engineering, Technical University of Catalonia, Barcelona, Spain.
Currently, he is a Postdoctoral Research Assistant in Department of Energy Technology, Aalborg University. His main research interests include distributed generation systems, microgrids and power quality issues of electrical systems.

Tomislav Dragicevic (S'09-M'13) received the M.E.E. and the Ph.D. degree from the Faculty of Electrical Engineering, Zagreb, Croatia, in 2009 and 2013, respectively. Since 2010, he has been actively cooperating in an industrial project related with design of electrical power supply for remote telecommunication stations. Since 2013 he has been a fulltime Post-Doc at Aalborg University in Denmark. His fields of interest include modeling, control and energy management of intelligent electric vehicle charging stations and other types of microgrids based on renewable energy sources and energy storage technologies.

Juan C. Vasquez (M'12-SM'15) received the B.S. degree in Electronics Engineering from Autonomous University of Manizales, Colombia in 2004 where he has been teaching courses on digital circuits, servo systems and flexible manufacturing systems. In 2009, He received his Ph.D degree in Automatic Control, Robotics and Computer Vision (ARV) from the Technical University of Catalonia, Barcelona, Spain in 2009 at the Department of Automatic Control Systems and Computer Engineering, from Technical University of Catalonia, Barcelona (Spain), where he worked as Post-doc Assistant and also teaching courses based on renewable energy systems. Since 2011, he has been an Assistant Professor in microgrids at the Institute of Energy Technology, Aalborg University, Aalborg, Denmark, where he is the co-responsible of the microgrids research program. His current research interests include operation, power management, hierarchical control and optimization applied to Distributed Generation in AC/DC microgrids. He is currently member of the Technical Committee on Renewable Energy Systems TC-RES.

Josep M. Guerrero (S'01-M'04-SM'08-FM'15) received the B.S. degree in telecommunications engineering, the M.S. degree in electronics engineering, and the Ph.D. degree in power electronics from the Technical University of Catalonia, Barcelona, in 1997, 2000 and 2003, respectively. Since 2011, he has been a Full Professor with the Department of Energy Technology, Aalborg University, Denmark, where he is responsible for the Microgrid Research Program. From 2012 he is a guest Professor at the Chinese Academy of Science and the Nanjing University of Aeronautics and Astronautics; from 2014 he is chair Professor in Shandong University; and from 2015 he is a distinguished guest Professor in Hunan University.
His research interests is oriented to different microgrid aspects, including power electronics, distributed energy-storage systems, hierarchical and cooperative control, energy management systems, and optimization of microgrids and islanded minigrids. Prof. Guerrero is an Associate Editor for the IEEE TRANSACTIONS ON POWER ELECTRONICS, the IEEE TRANSACTIONS ON INDUSTRIAL ELECTRONICS, and the IEEE Industrial Electronics Magazine, and an Editor for the IEEE TRANSACTIONS on SMART GRID and IEEE TRANSACTIONS on ENERGY CONVERSION. He has been Guest Editor of the IEEE TRANSACTIONS ON POWER ELECTRONICS Special Issues: Power Electronics for Wind Energy Conversion and Power Electronics for Microgrids; the IEEE TRANSACTIONS ON INDUSTRIAL ELECTRONICS Special Sections: Uninterruptible Power Supplies systems, Renewable Energy Systems, Distributed Generation and Microgrids, and Industrial Applications and Implementation Issues of the Kalman Filter; and the IEEE TRANSACTIONS on SMART GRID Special Issue on Smart DC Distribution Systems. He was the chair of the Renewable Energy Systems Technical Committee of the IEEE Industrial Electronics Society. In 2014 he was awarded by Thomson Reuters as Highly Cited Researcher, and in 2015 he was elevated as IEEE Fellow for his contributions on "distributed power systems and microgrids."